Eddy Diffusivity and Countergradient Transport in the Convective Atmospheric Boundary Layer

A. A. M. HOLTSLAG

Royal Netherlands Meteorological Institute (KNMI), De Bilt, The Netherlands

CHIN-HOH MOENG

National Center for Atmospheric Research, Boulder, Colorado*

(Manuscript received 29 August 1990, in final form 8 March 1991)

ABSTRACT

To describe the heat and scalar fluxes in the convective boundary layer, we propose expressions for eddy diffusivities and countergradient terms. The latter expressions can be used in a modified flux-gradient approach, which takes account for nonlocal convective vertical exchange. The results for heat are based on a derivation similar to that of Deardorff by utilizing the turbulent heat-flux equation, but the closure assumptions applied to the heat-flux budgets are different. As a result, the physical interpretation for the countergradient term differs; our countergradient term results from the third-moment transport effect, while Deardorff's results from the buoyancy production term. On the basis of our analysis, we are able to calculate an eddy diffusivity for heat, using large-eddy simulation results. The results are presented in the form of a similarity profile, using the convective velocity scale w_* and the inversion height z_i. It is shown that the latter profile is well behaved and that it matches the results of surface-layer theory. Using the top-down and bottom-up decomposition, we have generalized our findings for any scalar, such as the moisture field or an air pollution contaminant. We show that the eddy diffusivity profile for scalar C is sensitive to the entrainment-surface flux ratio of C. Therefore, a different scalar field should have a different eddy-diffusivity profile. The proposed expressions for the eddy diffusivities and the countergradient terms are easy to apply in (large-scale) atmospheric and diffusion models.

1. Introduction

In the upper half of the convective, atmospheric boundary layer (CABL), the upward transport of heat is typically accompanied by a slightly stable temperature gradient. This means that the heat transport is countergradient and that the usual flux-gradient approach is not appropriate (Deardorff 1966, 1972; Schumann 1987). The countergradient transport originates from large convective plumes (or eddies) that dominate the transport in the CABL. As such, the use of an eddy-diffusivity formulation based on local gradients alone (so-called *local K theory*) is not physical and of limited value (e.g., Ebert et al. 1989). Nevertheless, atmospheric models often utilize local K theory and neglect countergradient transport.

Deardorff (1972) derived the countergradient term for heat in the CABL by neglecting the transport term in the heat-flux equation. In this paper, we will derive a modified countergradient term by utilizing the recent results of large-eddy simulations (LES) by Moeng and Wyngaard (1989). We introduce an empirical parameterization for the transport term in the heat-flux equation and use the modified Rotta return-to-isotropy hypothesis by Moeng and Wyngaard (1986); this leads directly to a simple description of vertical heat transport.

In section 2, our results and those of Deardorff (1972) are compared with the LES data for heat transport. We also discuss matching of our results with those for the atmospheric surface layer.

In section 3, we extend our analysis to *top-down/bottom-up diffusion* (Wyngaard and Brost 1984) in which the impact on the diffusion of scalar fluxes at the surface and at the top of the CABL are distinguished. In previous studies it has been found that the eddy diffusivity of the bottom-up diffusion has a singularity in the midpart of the CABL, while the top-down diffusivity is well behaved (Moeng and Wyngaard 1984; Wyngaard 1987; Schumann 1989). Using a countergradient correction for the bottom-up diffusion of a scalar similar to the one for heat, we obtain a well-behaved diffusivity for the bottom-up field. Consequently, we are able to generalize our findings to the

* The National Center for Atmospheric Research is sponsored by the National Science Foundation.

Corresponding author address: Dr. Bert Holtslag, KNMI Research Division, P.O. Box 201, 3730 AE De Bilt, The Netherlands.

transport of any scalar, such as the specific humidity (q) or any other conservative species (C).

Both for heat and scalar diffusion, our findings combine local gradient transport and nonlocal countergradient transport. As such, they are easy to apply into (large-scale) atmospheric and diffusion models. Our results become a generalization of the proposals by Priestley and Swinbank (1947) and Troen and Mahrt (1986).

2. Transport of heat

a. The heat-flux equation

Under horizontally homogeneous conditions, the equation for the heat flux $\overline{w\theta}$ reads in the Boussinesq approximation as (e.g., Deardorff 1972)

$$\frac{\partial \overline{w\theta}}{\partial t} = -\frac{\partial \overline{w^2\theta}}{\partial z} - \overline{w^2}\frac{\partial \Theta}{\partial z} + \beta g \overline{\theta^2} - \frac{1}{\rho_0}\overline{\theta \frac{\partial p}{\partial z}}, \quad (1)$$

where θ is the potential temperature fluctuation, Θ is the mean value of the potential temperature, w is the vertical-velocity fluctuation, z is height, βg is the buoyancy parameter, ρ_0 is density of air at the reference state, p is the pressure fluctuation, and overbars denote ensemble averages. The terms on the right-hand side (rhs) of (1) are, in order, the turbulent transport term (denoted below by T), the mean-gradient production (M), the buoyant production (B), and the pressure covariance (P). Here we have included the minus signs in the definitions of T, M and P.

Figure 1, adopted from Moeng and Wyngaard (1989), shows the vertical profiles of the terms at the rhs of (1). The terms are normalized with the height of the CABL, z_i, the convective velocity scale, w_*, and the convective temperature scale, θ_*, where

$$w_* \equiv (\beta g \overline{w\theta_0} z_i)^{1/3}, \quad (2)$$

$$\theta_* \equiv \frac{\overline{w\theta_0}}{w_*}, \quad (3)$$

and $\overline{w\theta_0}$ is the kinematic surface heat flux. The statistics shown here are from $(96)^3$, wave-cutoff filtered simulations over a 5 km × 5 km × 2 km numerical domain. They are averaged over the horizontal plane and over about three large eddy turnover times z_i/w_*. In the LES we have $\overline{w\theta_0} \approx 0.24$ mK s^{-1}, $z_i \approx 1000$ m, $w_* \approx 2$ m s^{-1}, $\theta_* \approx 0.12$ K, and the friction velocity $u_* \approx 0.6$ m s^{-1}.

The transport term T of (1) is not small in comparison with the other terms. In many cases (i.e., Deardorff 1972), however, this term is neglected. In second-order closure modeling, T is often modeled with the downgradient diffusion assumption, but the latter is inappropriate owing to the dominant buoyancy effect (Moeng and Wyngaard 1989). The mean gradient term M changes sign in the mid CABL, where the buoyancy flux $\overline{w\theta}$ is positive, indicating the countergradient transport.

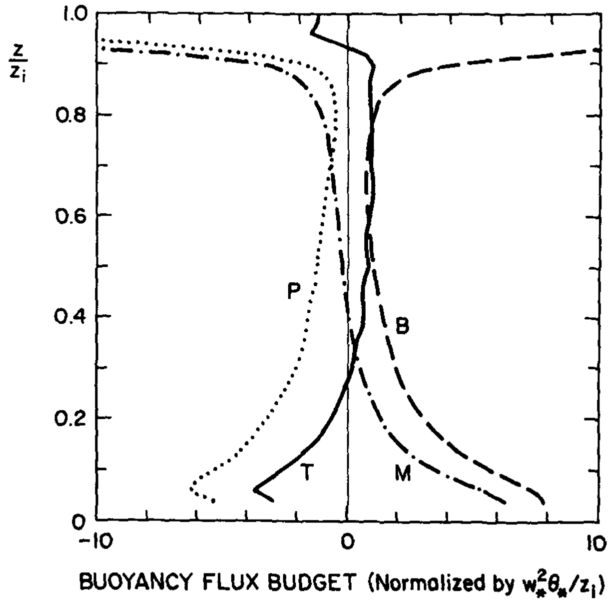

FIG. 1. The normalized terms at the rhs of the heat-flux equation (1), as a function of relative height (adopted from Moeng and Wyngaard 1989). The terms are defined in the text of section 2a.

Figure 1 suggests that T is larger than P by a nearly constant value throughout most of the CABL (i.e., $0.1 \leq z/z_i \leq 0.8$). We, therefore, empirically parameterize the transport term T as

$$T \approx P + b\frac{w_*^2\theta_*}{z_i}, \quad (4)$$

where $b \approx 2$. Lenschow et al. (1980; their Fig. 17) and Adrian et al. (1986; their Fig. 19) provide experimental data on T and P, which can be used for comparison. We have to realize, however, that both T and P are very hard to measure due to sampling problems. Moreover, in the cited studies the pressure term P is obtained as a residual term, which makes the outcome very sensitive for measuring errors. Nevertheless, T as obtained by Lenschow et al. and Adrian et al. is qualitatively similar to T in our Fig. 1. Our T is also in fair agreement with the large-eddy simulations of Schmidt (1988, his Fig. 18d, p. 75). Regarding the experimental uncertainty, we can not give a more detailed comparison at this moment. We realize that (4) is a very simple means to parameterize the transport term T, but we will accept it as a convenient closure assumption.

The pressure covariance term P can be modeled as (e.g., Crow 1968; Moeng and Wyngaard 1986)

$$P \equiv -\frac{1}{\rho_0}\overline{\theta\frac{\partial p}{\partial z}} = -a\beta g\overline{\theta^2} - \frac{\overline{w\theta}}{\tau}, \quad (5)$$

where τ is a return-to-isotropy time scale, and a is a constant. For isotropic turbulence, $a = 1/3$. For turbulence within the CABL, Moeng and Wyngaard (1986) obtained $a \approx 1/2$. Above the mixed layer, a may depend on the stability and structure of the inversion layer. Often, only the second term on the rhs of (5) is taken into account; it is known as the Rotta return-to-isotropy hypothesis. The first term on the rhs of (5) shows that P is directly related to the buoyant production rate $\beta g \overline{\theta^2}$. When (4) and (5) are substituted into (1), we obtain

$$\frac{\partial \overline{w\theta}}{\partial t} = -\overline{w^2}\frac{\partial \Theta}{\partial z} + (1-2a)\beta g \overline{\theta^2} - 2\frac{\overline{w\theta}}{\tau} + \frac{b w_*^2 \theta_*}{z_i}. \quad (6)$$

By adopting $a = 1/2$ of Moeng and Wyngaard (1986), the buoyant production term $\beta g \overline{\theta^2}$ disappears from (6). Then, in quasi-steady states, (6) becomes

$$\frac{\overline{w\theta}}{\tau} \approx -\frac{\overline{w^2}}{2}\frac{\partial \Theta}{\partial z} + \frac{b}{2}\frac{w_*^2 \theta_*}{z_i}. \quad (7)$$

For $a \neq 1/2$ we obtain an additional term at the rhs of (7), which is given by $(1/2 - a)\beta g \overline{\theta^2}$. In such cases the description for the heat flux is no longer as simple as we present here. Therefore (7) is restricted to turbulence within the CABL for which $a \approx 1/2$.

Although (7) is partly based on the simple empirical parameterization of (4), it is physically appealing. It shows that the heat flux depends on a local downgradient transport (first term on the rhs) and a nonlocal convective transport (second term on rhs). Therefore, the form of (7) is closely related to the original proposal by Priestley and Swinbank (1947), who found from mixing-length arguments that the heat-flux expression should contain a convective part in addition to the usual downgradient part. We note that the convective part of (7) arises from the turbulent transport term and that it is proportional to the surface heat flux $w_*\theta_*$ [see (3)]. Recently, Wyngaard and Weil (1991) obtained a very similar result as (7) through a kinematic derivation. Comparison of their findings with (7) suggests that the parameter b is proportional to the skewness S of the vertical turbulent velocity field ($S = \overline{w^3}/\overline{w^2}^{3/2}$). In the CABL the skewness is positive due to fast rising updrafts and slow descending downdrafts. In the absence of skewness (e.g., $b \to 0$), it is seen that (7) reduces to the usual downgradient diffusion concept.

b. Eddy diffusivities and countergradient terms

To facilitate a comparison with the previous results by Deardorff (1966, 1972), it is convenient to write (7) as

$$\overline{w\theta} = -K_H\left(\frac{\partial \Theta}{\partial z} - \gamma_\theta\right), \quad (8)$$

where in our case K_H and γ_θ are given by

$$K_H = \overline{w^2}\frac{\tau}{2}, \quad (9a)$$

and

$$\gamma_\theta = b\frac{w_*^2\theta_*}{\overline{w^2}z_i}. \quad (9b)$$

Here K_H and γ_θ can be interpreted as an eddy diffusivity and a countergradient term, respectively.

Deardorff (1972) obtained (8) by neglecting the transport term T in the heat-flux equation (1) and using (5) with $a = 0$. This means that he makes use of $P \equiv -\overline{w\theta}/\tau_D$, where τ_D is a time scale related to the turbulence energy and a mixing length. In that case, K_H and γ_θ are given by

$$K_H = \overline{w^2}\tau_D \quad (10a)$$

and

$$\gamma_\theta = \beta g \frac{\overline{\theta^2}}{\overline{w^2}}. \quad (10b)$$

The physical interpretation of the countergradient terms by (9b) and (10b) is very different. Equation (10b) comes from the buoyancy production term, while (9b) arises from the turbulent transport term by (4). We note that in Deardorff's (1966) paper a proper discussion of γ_θ in terms of the transport term in the *temperature variance equation* is given (see also Schumann 1987). We show here that the third-moment transport term in the *heat-flux equation* is also responsible for the countergradient term.

In Fig. 2, we compare the magnitudes of (9b) and (10b), where we have normalized γ_θ with θ_*/z_i and where all the turbulent quantities are obtained from the (resolved) LES data of Moeng and Wyngaard (1989). It is seen that the magnitude of the two expressions differs by a factor of two near $z/z_i \approx 0.7$ (or even more for $z/z_i < 0.2$), but that their general behavior is very similar despite the different physics. [Although, strictly speaking, our results on the basis of (4) apply only to $0.1 \leqslant z/z_i \leqslant 0.8$, we have extended the range in all figures below for illustration purposes.]

Figure 3 shows a comparison of the (normalized) eddy diffusivity obtained from (8) as

$$\frac{K_H}{w_* z_i} = \frac{-\overline{w\theta}/\overline{w\theta_0}}{(\partial\Theta/\partial z - \gamma_\theta)z_i/\theta_*}, \quad (11)$$

utilizing the LES data for $\partial\Theta/\partial z$, $\overline{w\theta}$ (both resolved and subgrid contributions) and using (9b) for γ_θ (see curve *a*). Also, the result of (9a) is given for comparison (curve *b*), where τ is directly calculated from the *turbulence–turbulence* component in the LES data (see Moeng and Wyngaard 1986). It is seen that the magnitudes of the K_H values by both calculations are of

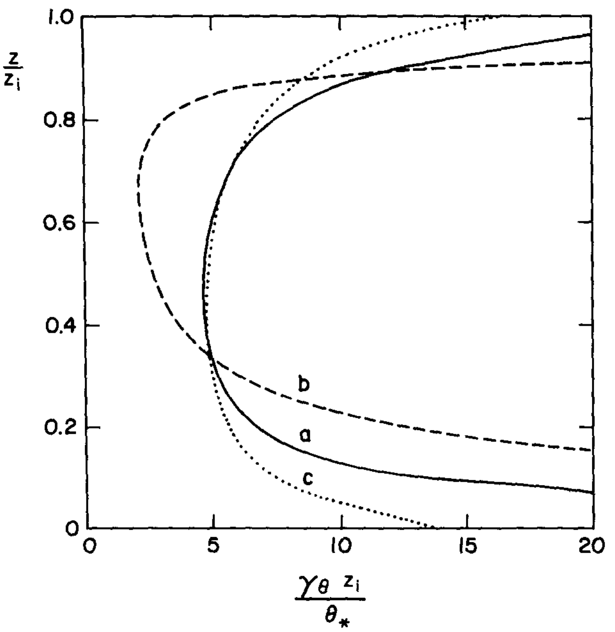

FIG. 2. Plot of the nondimensional countergradient term for heat, according to a: (9b), b: (10b), and c: (9b) with (15a).

the order of 0.1 in the mid part of the ABL. The result by (9a) shows an unexpected peak near $z/z_i \approx 0.1$ that is probably due to uncertainties in the calculation of τ near that height. Overall, Fig. 3 shows that (9a) is fairly consistent with the results of (11) and (9b).

In Fig. 3 (curve c), we have also shown the result for K_H, if (11) is combined with Deardorff's expression by (10b). It is seen that a singularity appears near $z/z_i \approx 0.7$, showing that the countergradient correction by (10b) is not sufficient to obtain a well-behaved profile for K_H (see also Fig. 2).

It is also illustrating to estimate the values of K_H and γ_θ in the central part of the CABL directly, where we may utilize

$$\overline{w^2} \approx c_1 w_*^2 \tag{12a}$$

and

$$\overline{\theta^2} \approx c_2 \theta_*^2. \tag{12b}$$

Here we estimate $c_1 \approx 0.4$ and $c_2 \approx 1$ for $z/z_i \approx 0.4$, as can be seen in Figs. 2 and 13 of Moeng and Wyngaard (1989) and Figs. 3 and 5 of Schmidt and Schumann (1989). Their figures are based on the results of large-eddy simulations, the AMTEX experiment (Lenshow et al. 1980), and convection tank experiments (Deardorff and Willis 1985) (see also Fig. 4 below).

In the CABL we have for $z/z_i \approx 0.4$, $\partial\Theta/\partial z \approx 0$ (see Fig. 1 where $M \approx 0$ for the latter height), and $\overline{w\theta}/w_*\theta_* \approx 0.5$, resulting with (7) and $b \approx 2$ in

$$\tau \approx 0.5 z_i/w_*. \tag{13a}$$

With (12a) and (13a), we can write (9a) as

$$K_H \approx 0.1 w_* z_i. \tag{13b}$$

The value of the eddy diffusivity by (13b) is on the order of the expected value for a diffusivity based on integral properties (e.g., Tennekes and Lumley 1972). The value is also consistent with the results in Fig. 3 from (9a), and (11) with (9b).

With (12a, b), we can write both (9b) and (10b) as

$$\gamma_\theta = c_4 \frac{\overline{w\theta_0}}{w_* z_i}, \tag{14a}$$

where $c_4 = b/c_1 \approx 5$ for (9b), and $c_4 = c_2/c_1 \approx 2.5$ for (10b). Using the values in the LES as typical values for $\overline{w\theta_0}$ ($\approx$0.24 mK s^{-1}), z_i ($\approx$1000 m), and w_* ($\approx$2 m s^{-1}), we obtain

$$\gamma_\theta \approx 0.6 \times 10^{-3}\ \mathrm{K\ m^{-1}} \tag{14b}$$

from (14a) with $c_4 = 5$. This value of γ_θ is close to the original value of 0.7×10^{-3} K m^{-1} for the countergradient term used by Deardorff (1966, 1972). Troen and Mahrt (1986) use (14a) for heat (and a similar one for moisture) with $c_4 = 10$ for $z/z_i \geqslant 0.1$; but Fig. 2 shows that γ_θ varies with height, and the coefficient $c_4 = 10$ seems too large by a factor of two in the mid part of the CABL.

c. Parameterizations and matching to the surface layer

For application of the present results, we parameterize $\overline{w^2}$ and our results in Fig. 3 for K_H. The vertical-

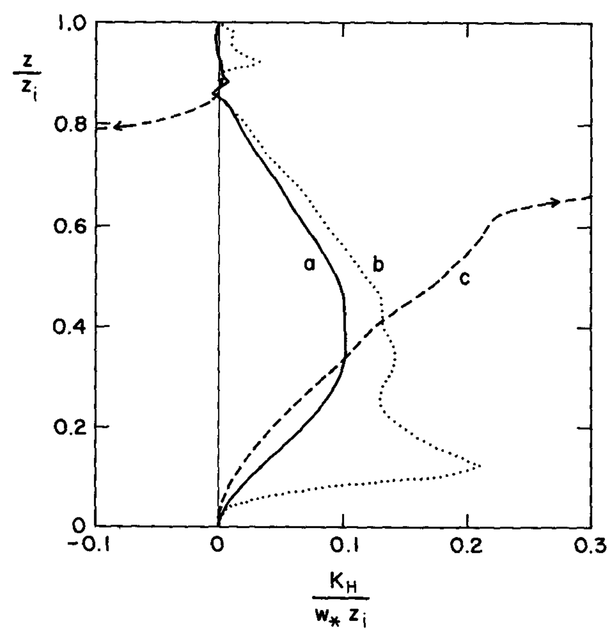

FIG. 3. Plot of the nondimensional eddy diffusivity for heat, according to a: (11) with (9b), b: (9a), and c: (11) with (10b).

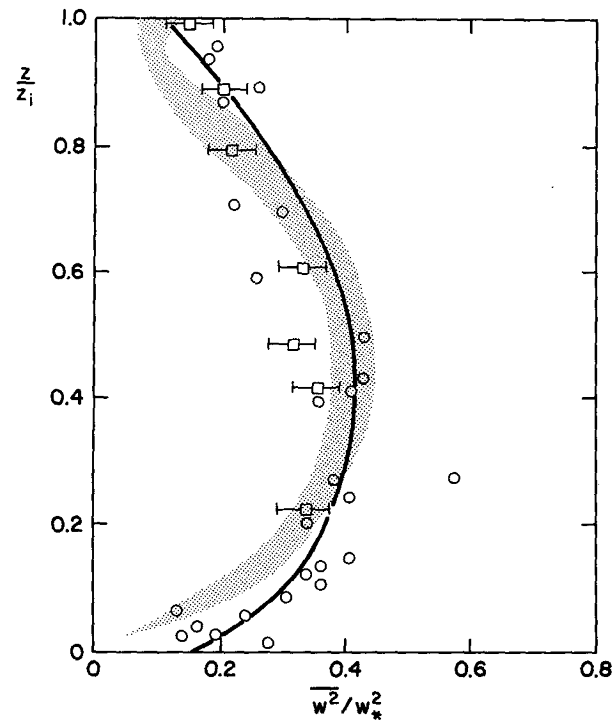

FIG. 4. The nondimensional vertical-velocity variance of (15a) (solid curve) in comparison with the $(96)^3$ LES data (shaded area; Moeng and Wyngaard 1989), the AMTEX data (circles; Lenschow et al. 1980), and convection tank experiments (squares; Deardorff and Willis 1985).

velocity variance is scaled by w_*^2 for the buoyancy-driven turbulence and by u_*^2 for the shear-driven turbulence. We, therefore, parameterize $\overline{w^2}$ as

$$(\overline{w^2})^{3/2} = \left[1.6u_*^2\left(1 - \frac{z}{z_i}\right)\right]^{3/2} + 1.2w_*^3\left(\frac{z}{z_i}\right)\left(1 - 0.9\frac{z}{z_i}\right)^{3/2} \quad (15a)$$

for $0 \leqslant z/z_i \leqslant 1$. The first term of (15a) reflects shear-driven turbulence, while the second term is for buoyancy-driven turbulence. Equation (15a) is based on the AMTEX field observations (Lenschow et al. 1980) and LES simulations (Moeng and Wyngaard 1989) for the buoyancy-dominated case. Equation (15a) is shown in Fig. 4 for $u_*/w_* = 0.3$, the value in the large eddy simulations. The latter is also close to the average value of $u_*/w_* \approx 0.25$ in AMTEX. Note that the LES results do not contain the subgrid contributions that are apparently significant for $z/z_i \leqslant 0.2$. It can be shown that (15a) also agrees reasonably with the LES data of Schmidt and Schumann (1989) for zero wind speed.

At the top of the surface layer ($z/z_i = 0.1$), we have with (15a)

$$\overline{w^2} = 1.44u_*^2\left(1 - 1.5\frac{z}{L}\right)^{2/3}, \quad (15b)$$

where L is the Monin–Obukhov length scale. The form of (15b) is consistent with the expression proposed by Panofsky et al. (1977), but the coefficients are in better agreement with the results by Højstrup (1982).

We have used (15a) in combination with (9b) to derive the countergradient term γ_θ, and the result is also given in Fig. 2. Since (15a) includes subgrid scale contributions, the resulting γ_θ is different from the LES result near the top and the surface. In Fig. 5 we show the K_H profile (curve b) that follows from (11), (9b), and the parameterized profile for $\overline{w^2}$ by (15a). The profile of curve a in Fig. 3 is given for reference (curve a). A curve fit to K_H (curve c) is given in Fig. 5 as

$$\frac{K_H}{w_* z_i} = \left(\frac{z}{z_i}\right)^{4/3}\left(1 - \frac{z}{z_i}\right)^2\left(1 + R_H\frac{z}{z_i}\right) \quad (16a)$$

for $0 \leqslant z/z_i \leqslant 1$. Here R_H is the ratio of entrainment flux to the surface flux for heat. In Fig. 5 we have taken $R_H = -0.2$ for curve c, which is the value of the LES data. Note that (16a) obeys the free-convection limit in the surface layer; e.g., $K_H \propto z^{4/3}$ for small z/z_i (e.g., Panofsky and Dutton 1984). In (16a), we have neglected the small contribution of shear production for simplicity. This means that (16a) is limited to convective cases for which $-z_i/L \geqslant 5$ or $u_*/w_* \leqslant 0.43$ (Holtslag and Nieuwstadt 1986).

The profile of (16a) can be compared with the expression by Troen and Mahrt (1986) showing

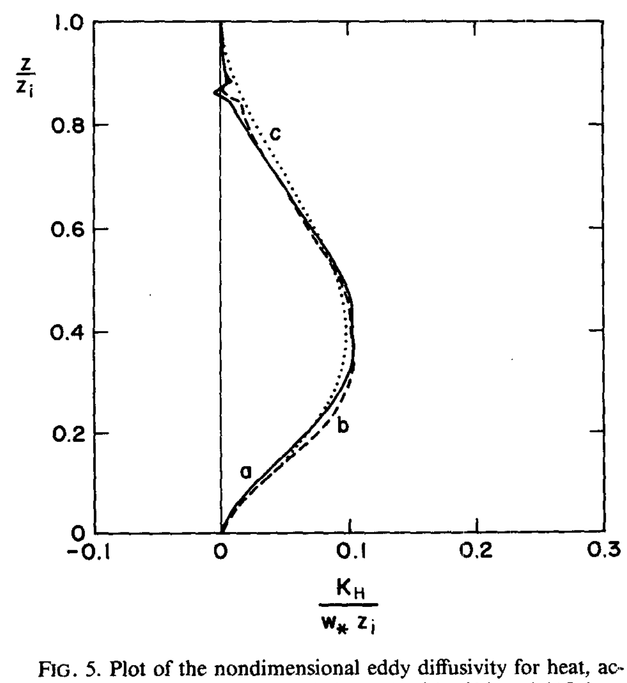

FIG. 5. Plot of the nondimensional eddy diffusivity for heat, according to a: as curve a in Fig. 3, b: (11) with (9b) and (15a), c: (16a) with $R_H = -0.2$.

$$\frac{K_H}{w_* z_i} = c\left(\frac{z}{z_i}\right)\left(1 - \frac{z}{z_i}\right)^2. \quad (16b)$$

Here c is a coefficient that depends on the Prandtl number (see Troen and Mahrt 1986; and Holtslag et al. 1990). It is seen that this equation does not obey the free-convection limit of the surface layer and that it is independent of the entrainment flux.

As a check of the above findings, we compare the outcome of (16a) with the results of surface-layer theory at the top of the surface layer. According to the latter theory, we may write (e.g., Dyer 1974; Högström 1988)

$$-\frac{\partial \Theta}{\partial z} = \frac{\overline{w\theta_0}}{k u_* z}\phi_h, \quad (17a)$$

where ϕ_h is obtained from observations as

$$\phi_h = \frac{1}{(1 - 16z/L)^{1/2}} \quad (17b)$$

for $0 \leqslant -z/L \leqslant 2$. As a result, we have with (3)

$$-\frac{z_i}{\theta_*}\frac{\partial \Theta}{\partial z} = \frac{w_*/u_*}{k(z/z_i)(1 - 16z/L)^{1/2}}. \quad (17c)$$

For $z/z_i = 0.1$ (the top of the surface layer) and $u_*/w_* = 0.3$ (the value in the LES), we obtain that $-z/L \approx 1.5$. With (11) and (17c) this results in $K_H/w_* z_i \approx 0.037$, where we have calculated $\gamma_\theta z_i/\theta_*$ with (9b) and (15b) and used $\overline{w\theta}/\overline{w\theta_0} = 0.9$. It appears that direct application of (16a) for $z/z_i = 0.1$ and $R_H = -0.2$ provides the same value for $K_H/w_* z_i$. This indicates that (16a) matches with the previously used ϕ_h function of (17b) (at least for the present value of u_*/w_*).

3. Scalar transport

a. Top-down and bottom-up diffusion

In the previous section, we have presented an eddy-diffusivity profile and a countergradient term for heat. A useful framework for further analysis of the results is to consider so-called top-down and bottom-up scalars (Wyngaard and Brost 1984; Moeng and Wyngaard 1984; 1989). Here top-down diffusion is driven by the entrainment flux, with a zero surface flux for the scalar flux; and the bottom-up diffusion is driven by the surface flux, with a zero entrainment flux for the scalar involved. Similarly with (8), we write for the bottom-up case

$$\overline{wc_b} = -K_b\left(\frac{\partial C_b}{\partial z} - \gamma_b\right), \quad (18a)$$

and for the top-down case

$$\overline{wc_t} = -K_t\left(\frac{\partial C_t}{\partial z} - \gamma_t\right), \quad (18b)$$

where in analogy with (9b) we write

$$\gamma_b = b_b\frac{w_*\overline{wc_0}}{\overline{w^2}z_i} \quad (19a)$$

and

$$\gamma_t = b_t\frac{w_*\overline{wc_1}}{\overline{w^2}z_i}. \quad (19b)$$

Here C_b and C_t are the mean concentrations of the bottom-up and top-down scalar, $\overline{wc_0}$ is the surface flux of the bottom-up scalar, and $\overline{wc_1}$ is the entrainment flux of the top-down scalar. Since in quasi-steady conditions the top-down and bottom-up fluxes are linear in height, i.e., $\overline{wc_b} = (1 - z/z_i)\overline{wc_0}$ and $\overline{wc_t} = (z/z_i)\overline{wc_1}$ (Wyngaard 1987), we have with (18) and (19)

$$\frac{K_b}{w_* z_i} = \frac{(1 - z/z_i)}{g_b + b_b w_*^2/\overline{w^2}} \quad (20a)$$

and

$$\frac{K_t}{w_* z_i} = \frac{z/z_i}{g_t + b_t w_*^2/\overline{w^2}} \quad (20b)$$

for $0 \leqslant z/z_i \leqslant 1$. The gradient functions g_b and g_t are the vertical gradients of C_b and C_t normalized by $-\overline{wc_0}/w_* z_i$ and $-\overline{wc_1}/w_* z_i$, respectively.

The top-down flux budgets given by Moeng and Wyngaard (1984, Fig. 7) suggest that the turbulent transport and pressure-covariance terms in the top-down flux budgets, i.e., the equivalence of the first and the fourth terms at the rhs of (1) for the top-down scalar, are about the same in most of the PBL. Therefore, we empirically set $b_t = 0$. For the bottom-up flux budget, the transport term is larger than the pressure term by a factor close to that shown in (4). Thus, we empirically set $b_b = b\,(\approx 2)$. Note that due to the term $b_b w_*^2/\overline{w^2}$ in the denominator of (20a), our definition of K_b differs from the one in previous studies by Wyngaard and Brost (1984), Moeng and Wyngaard (1984), and Schumann (1989), while the result of (20b) for K_t with $b_t = 0$ is the same.

Figures 6 and 7 plot the K profiles given by (20a, b) using the $(96)^3$ LES results for g_b, g_t, and $\overline{w^2}/w_*^2$ calculated by (15a). Due to the additional term $b_b w_*^2/\overline{w^2}$ in the denominator of (20a), the expression for K_b is well behaved and has a smaller magnitude. Neglecting the additional term leads to a K_b-profile that has a singularity in the central part of the CABL and becomes negative in the upper part of the CABL (see Wyngaard 1987; and Schumann 1989). This is due to $g_b \rightarrow 0$ for $z/z_i \approx 0.4$. Since we have set $b_t = 0$ in (20b) [and therefore also $\gamma_t = 0$ in (19b)], it appears that our K_t compares well with the LES data of Schumann (1989, his Fig. 4) for $0.2 \leqslant z/z_i \leqslant 1$. It can be seen that our modified K_b is a factor of two smaller

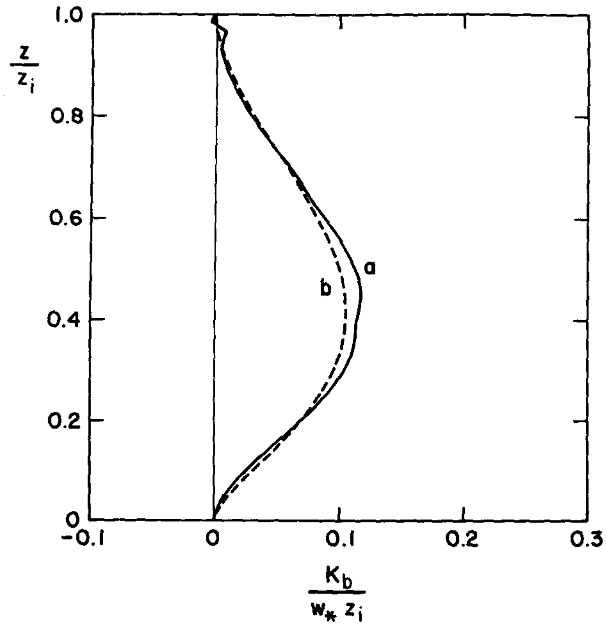

FIG. 6. Plot of the nondimensional eddy diffusivity for bottom-up transport, according to a: (20a), b: (21a).

than K_t, which together with the different findings for γ_b and γ_t illustrates the asymmetry in top-down and bottom-up diffusion (e.g., Wyngaard 1987; Schumann 1989; Wyngaard and Weil 1991).

We can curve fit the K_b and K_t profiles of Figs. 6 and 7 as

$$\frac{K_b}{w_* z_i} = \left(\frac{z}{z_i}\right)^{4/3}\left(1 - \frac{z}{z_i}\right)^2 \tag{21a}$$

and

$$\frac{K_t}{w_* z_i} = 7\left(\frac{z}{z_i}\right)^2\left(1 - \frac{z}{z_i}\right)^3 \tag{21b}$$

for $0 \leqslant z/z_i \leqslant 1$. We note that (21a) is consistent with (16a) for $R_H = 0$, and that both (21a, b) peak at $z/z_i = 0.4$.

b. Generalization

In quasi-steady conditions, any scalar flux $\overline{wc}$ may be written as a linear combination of the surface flux and the entrainment flux (see Wyngaard 1987):

$$\overline{wc} = \left(1 - \frac{z}{z_i}\right)\overline{wc}_0 + \frac{z}{z_i}\overline{wc}_1, \tag{22}$$

and the mean gradient $\partial C/\partial z$ can be written in terms of g_b and g_t as

$$\frac{\partial C}{\partial z} = \frac{-(\overline{wc}_0 g_b + \overline{wc}_1 g_t)}{w_* z_i}. \tag{23}$$

Writing

$$\overline{wc} = -K_c\left(\frac{\partial C}{\partial z} - \gamma_c\right), \tag{24}$$

and using (19a), (22), and (23), we obtain the eddy diffusivity for any scalar K_c as

$$\frac{K_c}{w_* z_i} = \frac{(1 - z/z_i) + R_c z/z_i}{g_b + R_c g_t + b_b w_*^2/\overline{w^2}}, \tag{25a}$$

where $R_c \equiv \overline{wc}_1/\overline{wc}_0$ is the entrainment-surface flux ratio of the scalar C. Here we set $b_t = 0$, as mentioned in section 3a. Using (20a) and (20b), we then rewrite (25a) as

$$K_c = \frac{(1 - z/z_i + R_c z/z_i)K_b K_t}{(1 - z/z_i)K_t + R_c(z/z_i)K_b} \tag{25b}$$

for $0 \leqslant z/z_i \leqslant 1$ and $R_c \geqslant 0$. Unlike the K theory, our eddy diffusivity profile depends on the ratio of the surface and entrainment fluxes of C. We plot normalized K_c profiles by (25b) for different R_c ratios in Fig. 8 [using the parameterized profiles by (21a, b) as well]: $R_c = 0$ retains the *bottom-up* result, and $R_c = 0.5$, 1.0, 1.5 are typical values for entrainment of moisture. For comparison we have also included the *top-down* result (21b), which follows from (25b) for $R_c \rightarrow \infty$. Overall, it is seen that the impact of the entrainment flux cannot be neglected and that K_c increases with increasing values of R_c.

For negative values of R_c (e.g., heat transport), the application of (25b) is restricted to cases for which the relative height reads as $z/z_i < 1/(1 - R_c)$ (=0.83 for

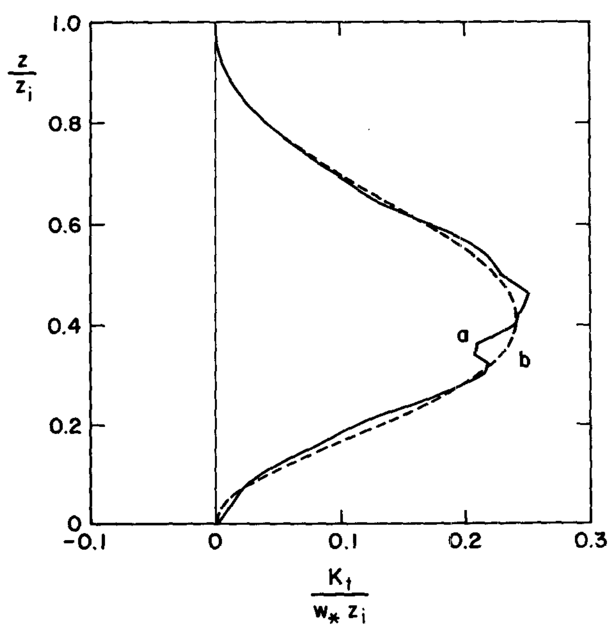

FIG. 7. Plot of the nondimensional eddy diffusivity for top-down transport, according to a: (20b), b: (21b).

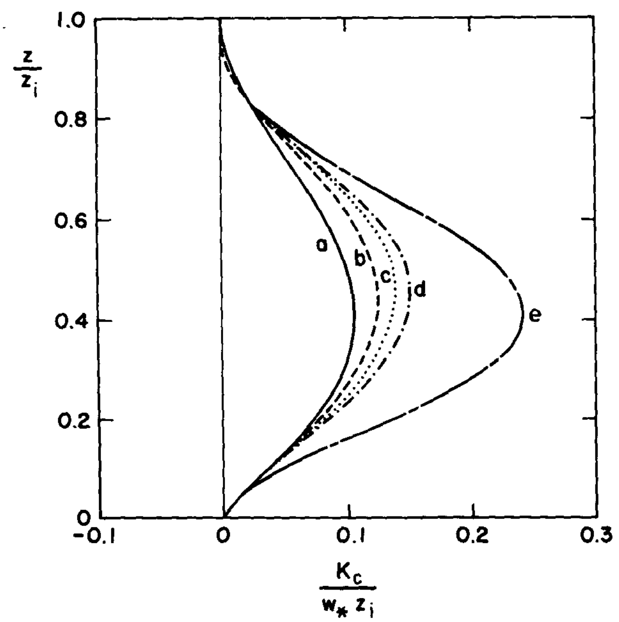

FIG. 8. Plot of the nondimensional eddy diffusivity for scalar transport by (25b) with (21a, b), for varying values of the entrainment-surface flux ratio R_c, namely a: 0, b: 0.5, c: 1, d: 1.5, e: ∞.

$R_c = -0.2$). Therefore, we propose to use (16a) for $-1 < R_c < 0$ (in which case the subscript H is replaced by the subscript c).

Since we have set b_t of (19b) to zero, we then write the countergradient term γ_c of (24) in a similar way as (9b); e.g.,

$$\gamma_c = b \frac{w_* \overline{wc}_0}{\overline{w^2} z_i}, \quad (26)$$

where again $b \approx 2$. As expected, γ_c vanishes in the neutral limit (e.g., $w_* = 0$) despite the value of the scalar flux at the surface.

4. Discussion and summary

The vertical exchange of heat and scalars in the convective, atmospheric boundary layer (CABL) is dominated by fast rising updrafts and slower descending downdrafts. To describe this nonlocal transport in the stationary, horizontally homogeneous CABL, we parameterize the pressure-covariance terms (P) and the transport terms (T) in the heat-flux equation and in the flux equations for the top-down and bottom-up scalars. This leads directly to (modified) descriptions for countergradient terms in the flux-gradient approach. As such, we extend the work by Deardorff (1972), who derived the countergradient term for heat from the buoyancy production term in the heat flux equation. Since Deardorff neglected the transport term in the heat-flux equation, our physical interpretation of the countergradient term differs from his; our countergradient term results from the third-moment transport effect. However, in Deardorff (1966) a proper discussion of the countergradient term is given by considering the transport term in the temperature variance equation. The outcome of our parameterization is physically appealing and consistent with previous independent derivations (Priestley and Swinbank 1947; Wyngaard and Weil 1991).

Using data of the large-eddy simulation by Moeng and Wyngaard (1989), we obtain expressions for the eddy diffusivities of heat, and top-down and bottom-up scalar diffusion. The expressions for the eddy diffusivities of heat and bottom-up scalar diffusion are well behaved due to the incorporation of the countergradient correction terms in the flux-gradient approach. However, it appears that the top-down scalar diffusivity is well behaved without countergradient correction. The latter is in agreement with independent LES data of Schumann (1989). We also obtain that the diffusivity for heat obeys the free convection limit in the surface layer and that its numerical value at the top of the surface layer is consistent with the usual surface-layer similarity function for the temperature gradient.

We use our findings for top-down and bottom-up scalar diffusion to generalize the description for scalar transport. It appears that in the generalized formula the eddy diffusivity depends on the entrainment-surface flux ratio. Therefore, a different scalar field should have a different eddy-diffusivity profile. As such, our results are a generalization of those by Priestley and Swinbank (1947) and Troen and Mahrt (1986). Our findings are described as profile functions of dimensionless height by applying the usual similarity parameters of the CABL (e.g., Holtslag and Nieuwstadt 1986). Consequently, our results can be used to describe the nonlocal convective exchange of heat and scalars. They may serve as simple, as well as physical, realistic alternatives to the transilient turbulence concept (Stull 1984; Ebert et al 1989).

The present descriptions for the eddy diffusivities and countergradient terms are suitable for application in (large-scale) atmospheric and diffusion models. As such we aim only at modeling of the mean quantities. That such descriptions are useful has been demonstrated by Holtslag et al. (1990). To derive the eddy diffusivities for heat and scalar transport, we can use (16a) and (25b). The corresponding countergradient terms are given by (9b) and (26). A suitable formulation for the boundary layer height z_i is given by Troen and Mahrt (1986).

The actual application of the present results and comparison with field data is beyond the goal of this paper and will be the subject of further study. We expect, however, that the present approach will result in physically more realistic vertical profiles for heat and scalars. For example, a model based on a local K approach without countergradient terms will lead to a superadiabatic temperature profile over a deeper layer than typically observed. In such an approach this is the only way to maintain the upward heat (and scalar) transport from the surface. Consequently, the temperature near the top of the CABL may be underestimated by 1 K or more (see also Deardorff 1972), and the scalar profiles will also be affected.

Acknowledgments. We are grateful to Drs. A. Andren, D. Lenschow, L. Mahrt, U. Schumann, J. Weil, J. Wyngaard, and an unknown referee for useful discussions and comments on an earlier draft of this paper. This paper has been prepared while the first author was a visiting scientist at NCAR, for which he acknowledges financial support and for which he thanks D. Lenschow and J. Wyngaard for making the arrangements. Fran Huth is thanked for editing the paper.

REFERENCES

Adrian, R. J., R. T. D. S. Ferreira and T. Boberg, 1986: A review of turbulent thermal convection in wide horizontal fluid layers. *Exper. in Fluids,* **4,** 121–141.

Crow, S. C., 1968: Visco-elastic properties of fine-grained incompressible turbulence. *J. Fluid Mech.,* **33,** 1–20.

Deardorff, J. W., 1966: The counter-gradient heat flux in the lower atmosphere and in the laboratory. *J. Atmos. Sci.,* **23,** 503–506.

——, 1972: Theoretical expression for the counter-gradient vertical heat flux. *J. Geophys. Res.,* **77,** 5900–5904.

——, and G. E. Willis, 1985: Further results from a laboratory model of the convective planetary boundary layer. *Bound.-Layer Meteorol.,* **32,** 205–236.

Dyer, A. J., 1974: A review of flux-profile relationships. *Bound.-Layer Meteor.,* **7,** 363–372.

Holtslag, A. A. M., and F. T. M. Nieuwstadt, 1986: Scaling the atmospheric boundary layer. *Bound.-Layer Meteor.,* **36,** 201–209.

——, E. I. F. de Bruijn and H.-L. Pan, 1990: A high resolution air mass transformation model for short range weather forecasting. *Mon. Wea. Rev.,* **118,** 1561–1575.

Ebert, E. E., U. Schumann and R. B. Stull, 1989: Nonlocal turbulent mixing in the convective boundary layer evaluated from large-eddy simulation. *J. Atmos. Sci.,* **46,** 2178–2207.

Højstrup, J., 1982: Velocity spectra in the unstable planetary boundary layer. *J. Atmos. Sci.,* **39,** 2239–2248.

Lenschow, D. H., J. C. Wyngaard and W. T. Pennell, 1980: Mean-field and second-moment budgets in a baroclinic, convective boundary layer. *J. Atmos. Sci.,* **37,** 1313–1326.

Moeng, C.-H., and J. C. Wyngaard, 1984: Statistics of conservative scalars in the convective boundary layer. *J. Atmos. Sci.,* **41,** 3161–3169.

——, and ——, 1986: An analysis of closures for pressure-scalar covariances in the convective boundary layer. *J. Atmos. Sci.,* **43,** 2499–2513.

——, and ——, 1989: Evaluation of turbulent transport and dissipation closures in second-order modeling. *J. Atmos. Sci.,* **46,** 2311–2330.

Panofsky, H. A., and J. A. Dutton, 1984: *Atmospheric Turbulence; Models and Methods for Engineering Applications.* Wiley & Sons, 397 pp.

——, H. Tennekes, D. H. Lenschow and J. C. Wyngaard, 1977: The characteristics of turbulent velocity components in the surface layer under convective conditions. *Bound.-Layer Meteorol.,* **11,** 355–361.

Priestley, C. H. B., and W. C. Swinbank, 1947: Vertical transport of heat by turbulence in the atmosphere. *Proc. Roy. Soc. London,* **A189,** 543–561.

Schmidt, H., 1988: Large-eddy simulation of convective boundary layers (in German), Thesis, University of München. [Available as report DFVLR-FB 88-30 from DLR, P.O. Box 906058, D-5000 Köln 90, Germany.]

——, and U. Schumann, 1989: Coherent structure of the convective boundary layer derived from large-eddy simulations. *J. Fluid Mech.,* **200,** 511–562.

Schumann, U., 1987: The counter-gradient heat flux in turbulent stratified flows. *Nuclear Engineering and Design,* **100,** 255–262.

——, 1989: Large-eddy simulation of turbulent diffusion with chemical reactions in the convective boundary layer. *Atmos. Environ.* **23,** 1713–1727.

Stull, R. B., 1984: Transilient turbulence theory. Part I: The concept of eddy mixing across finite distances. *J. Atmos. Sci.,* **41,** 3351–3367.

Tennekes, H., and J. L. Lumley, 1972: *A First Course In Turbulence.* MIT Press, 300 pp.

Troen, I., and L. Mahrt, 1986: A simple model of the atmospheric boundary layer; Sensitivity to surface evaporation. *Bound.-Layer Meteor.,* **37,** 129–148.

Wyngaard, J. C., 1987: A physical mechanism for the asymmetry in top-down and bottom-up diffusion. *J. Atmos. Sci.,* **44,** 1083–1087.

——, and R. A. Brost, 1984: Top-down and bottom-up diffusion of a scalar in the convective boundary layer. *J. Atmos. Sci.,* **41,** 102–112.

——, and J. C. Weil, 1991: Transport asymmetry in skewed turbulence. *Physics of Fluids* **A3,** 155–162.